Zwitterionic Metallocenes Derived from *rac* and *meso*-Ethylenebisindenyl Zirconocene Olefin Complexes and Pentafluorophenyl-Substituted Boranes

Lawrence W. M. Lee,[†] Warren E. Piers,*[,†,1] Masood Parvez,[†] Steven J. Rettig,[‡,2] and Victor G. Young, Jr.[§]

Department of Chemistry, University of Calgary, 2500 University Drive N. W., Calgary, Alberta, T2N 1N4, Canada, Department of Chemistry, University of British Columbia, 2036 Main Mall, Vancouver, British Columbia, V6T 1Y6, Canada, and Department of Chemistry, University of Minnesota, 207 Pleasant Street S. E., Minneapolis, Minnesota 55455.

Received May 21, 1999

Trimethylphosphine-stabilized ethylene complexes **1** of the ethylenebisindenyl-supported zirconocene fragment are prepared via magnesium reduction of *rac*-(EBI)$ZrCl_2$ in the presence of ethylene and PMe_3. When the reaction is halted after 6 h, good yields of a mixture containing *rac*-(EBI)Zr(η^2-CH_2=CH_2)PMe_3, ***rac*-1**, and the racemic diastereomer of the zirconacyclopentane derivative (EBI)Zr(η^2-$CH_2CH_2CH_2CH_2$), ***rac*-2**, are obtained. This mixture may be converted to pure ***rac*-1** if treated with excess PMe_3. If the magnesium reduction of *rac*-(EBI)$ZrCl_2$ is left for 3 days in the presence of magnesium chloride, complete epimerization to ***meso*-1** is observed. Thus, both diastereomers of **1** are available. Compounds ***meso*-1** and ***rac*-2** have been characterized crystallographically. The coordinated ethylene ligands in compounds **1** are susceptible to electrophilic attack by the pentafluorophenyl-substituted boranes $HB(C_6F_5)_2$ and $B(C_6F_5)_3$, forming zwitterionic metallocene products. For reactions involving $HB(C_6F_5)_2$, the products ***meso*-3** and ***rac*-3** are characterized by a strong zirconium−hydrido borate interaction, as well as a weak Zr−C_β bonding. In addition to complete solution characterization, the structure of ***meso*-3** was determined crystallographically. Upon treatment of ***rac*-1** with $B(C_6F_5)_3$, a more charge-separated zwitterion, ***rac*-4**, was formed. In addition to retaining its PMe_3 ligand, the complex is stabilized by a strong β-CH_2 interaction, as determined by X-ray crystallography and NMR spectroscopy. Structural comparisons between the compounds reported herein and previous examples in metallocene chemistry are presented.

Introduction

Metallocene[3,4] and half-metallocene[5] compounds of the group 4 metals are important industrial catalysts for the production of various polyolefin commodities. In the presence of a suitable Lewis acid activator, the neutral metallocenes Cp_2MR_2 or $CpMR_3$ are transformed into the catalytically active cationic species $[Cp_nMR_m]^+[AR]^-$.[6] In these compounds, the extent of ion−ion interaction can have a profound effect on both the activity and the stability of the catalyst.[7] Generally, as the anion becomes more weakly coordinating, the activity of the catalyst increases, but the stability (particularly in the absence of monomer) decreases. Thus, catalyst design must strike a balance between activity and stability.

Cation−anion interactions may be to some degree controlled through the use of zwitterionic catalysts, in which the anion is covalently sequestered to some portion of the catalyst molecular framework.[8] One strategy for preparing such compounds has been the electrophilic attack of coordinated π-ligands such as butadiene[9] or olefins. Accordingly, we have examined

[†] University of Calgary.
[‡] University of British Columbia.
[§] University of Minnesota.

(1) To whom correspondence may be addressed. Phone: (403)-220-5746. Fax: (403)-289-9488. E-mail: wpiers@ucalgary.ca.

(2) Deceased, October 27, 1998. This paper is dedicated to the memory of Steve Rettig, friend and crystallographer par excellence.

(3) Reviews: (a) Resconi, L.; Camurati, I.; Sudmeijer, O. *Top. Catal.* **1999**, *7*, 145. (b) Bochmann, M. *J. Chem. Soc., Dalton Trans.* **1996**, 255. (c) Brintzinger, H. H.; Fischer, D.; Mulhaupt, R.; Rieger, B.; Waymouth, R. M. *Angew. Chem., Int. Ed. Engl.* **1995**, *34*, 1143. (d) Mohring, P. C.; Coville, N. J. *J. Organomet. Chem.* **1994**, *479*, 1. (e) Marks, T. J. *Acc. Chem. Res.* **1992**, *25*, 57.

(4) Recent references: (a) Herzog, T. A.; Zubris, D. L.; Bercaw, J. E. *J. Am. Chem. Soc.* **1996**, *118*, 11988. (b) Maciejewski-Petoff, J. L.; Bruce, M. D.; Waymouth, R. M.; Masood, A.; Lal, T. K.; Quan, R. W.; Behrend, S. J. *Organometallics* **1997**, *16*, 5909. (c) Bruce, M. D.; Coates, G. W.; Hauptman, E.; Waymouth, R. M.; Ziller, J. W. *J. Am. Chem. Soc.* **1997**, *119*, 11174. (d) Bravakis, A. M.; Baily, L. E.; Pigeon, M.; Collins, S. *Macromolecules* **1998**, *31*, 1000. (e) Dietrich, U.; Hackmann, M.; Rieger, B.; Klinga, M.; Leskelä, M. *J. Am. Chem. Soc.* **1999**, *121*, 4348.

(5) (a) Ewart, S. W.; Baird, M. C. *Top. Catal.* **1999**, *7*, 1. (b) McKnight, A. L.; Waymouth, R. M. *Chem. Rev.* **1998**, *98*, 2587.

(6) Jordan, R. F. *Adv. Organomet. Chem.* **1991**, *32*, 325.

(7) a) Chen, Y.-X.; Metz, M. V.; Li, L.; Stern, C. L.; Marks, T. J. *J. Am. Chem. Soc.* **1998**, *120*, 6287, and references therein. (b) Luo, L.; Marks, T. J. *Top. Catal.* **1999**, *7*, 97.

(8) (a) Bochmann, M. *Top. Catal.* **1999**, *7*, 9. (b) Piers, W. E. *Chem. Eur. J.* **1998**, *4*, 13.

10.1021/om990383d CCC: $18.00
Publication on Web 08/20/1999

the reactions of the perfluoroaryl-substituted boranes $HB(C_6F_5)_2$[10] and $B(C_6F_5)_3$[11] with zirconocene olefin complexes $Cp_2Zr(\eta^2\text{-}CH_2{=}CHR)(PR_3)$ (Scheme 1).[12] In general, the boranes attack the most sterically accessible lobes of the zirconocene HOMO, which in these systems is largely associated with the coordinated olefin ligand. In the resulting zwitterionic products, more complete charge separation is observed in the reactions involving $B(C_6F_5)_3$, since in the $HB(C_6F_5)_2$-derived products there is a strong hydridoborate−zirconium interaction present. Accordingly, the former compound is a much better ethylene polymerization initiator than the latter.

Since significant enhancement in olefin polymerization activity can be observed upon partial substitution of the Cp ring in metallocene catalysts,[13] we have extended these studies to include *ansa*-zirconocene olefin complexes that are supported by the ethylenebisindenyl ligand framework.[14] Both *rac* and *meso* isomers of $(EBI)Zr(\eta^2\text{-}CH_2{=}CH_2)PMe_3$ have been prepared and their reactions with the two highly electrophilic boranes examined. The reactions produce products structurally similar to those observed in the parent bis-Cp system.[12] In addition to providing more structural examples of this class of zwitterions, the work described herein provides a protocol for generating a synthon of "*rac*-(EBI)Zr" without epimerization, significant given the importance of "Cp_2Zr" in various coupling reactions.[15]

Results and Discussion

Zirconocene Olefin Precursors. Phosphine-stabilized olefin complexes of the (EBI)Zr molecular fragment were not to our knowledge reported prior to this study, so we first developed the chemistry necessary to provide the required precursors for reaction with the boranes. In the parent bis-Cp system, the method of choice for preparing olefin complexes is to allow dialkyl compounds with β-hydrogens, $Cp_2Zr(CH_2CHR)_2$, to thermally decompose in the presence of a trapping phosphine ligand.[16] While this process is chemically quite complex,[17] it generally leads to the desired compounds in excellent yields.

Scheme 1

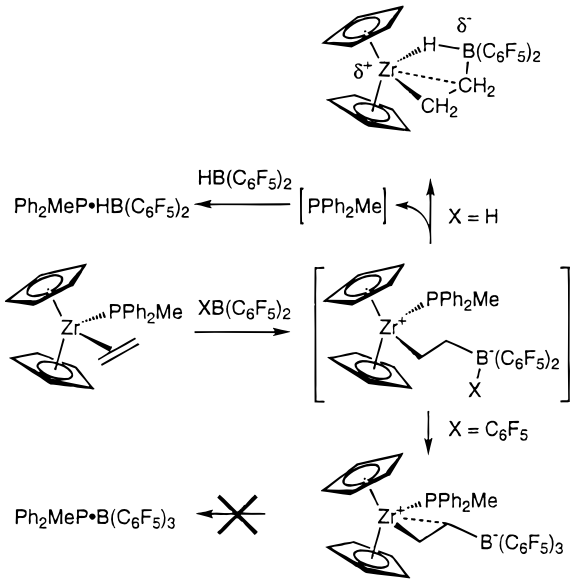

In the reaction of *rac*-$(EBI)ZrCl_2$ with EtLi or EtMgBr, although the desired diethyl species is generated, its formation is accompanied by a significant amount of epimerization.[18] Thus, mixtures of *rac* and *meso* diastereomers of the η^2-ethylene complex are formed in these reactions, and physical separation is difficult. Alkyllithium and Grignard reagents and even lithium or magnesium salts are known to promote epimerization of *ansa*-metallocenes[19] presumably via cleavage of the M−Cp bond followed by recoordination of the opposite enantioface of the cyclopentadienyl ring. Unfortunately, we could not devise conditions that allowed for production of diastereomerically pure (EBI)Zr−ethylene complexes using this methodology.

A milder method for this purpose, using magnesium reduction, was found; this chemistry is summarized in Scheme 2. When *rac*-$(EBI)ZrCl_2$ is treated with magnesium powder in the presence of ethylene and trimethylphosphine, reduction of the dichloride and trapping of the putative "*rac*-(EBI)Zr" fragment take place without competing epimerization of the *ansa*-metallocene. Thus, if the reaction is halted after 6 h, a mixture of the two compounds *rac*-$(EBI)Zr(\eta^2\text{-}CH_2{=}CH_2)PMe_3$, ***rac*-1**, and the metallacyclopentane complex *rac*-$(EBI)Zr(CH_2CH_2CH_2CH_2)$, ***rac*-2**, is formed in good yield. No trace of *meso* isomers could be detected by proton NMR spectroscopy, and once separated from the $MgCl_2$ byproduct, these compounds are stable toward diastereoisomerization. The zirconacycloalkane products ***rac*-1** and ***rac*-2** are interconvertable by treatment with either excess PMe_3 or ethylene (eq 1). Thus, as described in

(9) (a) Karl, J.; Dahlmann, M.; Erker, G.; Bergander, K. *J. Am. Chem. Soc.* **1998**, *120*, 5643. (b) Karl, J.; Erker, G. *J. Mol. Cat.* **1998**, *128*, 85. (c) Karl, J.; Erker, G. *Chem. Ber.* **1997**, *130*, 1261. (d) Karl, J.; Erker, G.; Fröhlich, R. *J. Am. Chem. Soc.* **1997**, *119*, 11165. (e) Karl, J.; Erker, G.; Fröhlich, R. *J. Organomet. Chem.* **1997**, *535*, 59. (f) Temme, B.; Karl, J.; Erker, G. *Chem. Eur. J.* **1996**, *2*, 919. (g) Temme, B.; Erker, G.; Karl, J.; Luftmann, H.; Fröhlich, R.; Kotila, S. *Angew. Chem., Int. Ed. Engl.* **1995**, *34*, 1755.

(10) (a) Parks, D. J.; Piers, W. E.; Yap, G. P. A. *Organometallics* **1998**, *17*, 5492. (b) Piers, W. E.; Spence, R. E. v. H. U.S. Patent 5,496,960, March 5, 1996.

(11) (a) Massey, A. G.; Park, A. J. *J. Organomet. Chem.* **1966**, *5*, 218. (b) Piers, W. E.; Chivers, T. *Chem. Soc. Rev.* **1997**, 345.

(12) (a) Sun, Y.; Piers, W. E.; Rettig, S. J. *Organometallics* **1996**, *15*, 4110. (b) Sun, Y.; Piers, W. E.; Rettig, S. J. *Chem. Commun.* **1998**, 127. (c) Piers, W. E.; Sun, Y.; Lee, L. W. M. *Top. Catal.* **1999**, *7*, 133.

(13) (a) Lee, I.-M.; Gauthier, W. J.; Ball, J. M.; Iyengar, B.; Collins, S. *Organometallics* **1992**, *11*, 2115. (b) Piccolrovazzi, N.; Pino, P.; Consiglio, G.; Sironi, A.; Moret, M. *Organometallics* **1990**, *9*, 3098.

(14) (a) Wild, F. R. W. P.; Zsolnai, L.; Huttner, G.; Brintzinger, H. H. *J. Organomet. Chem.* **1982**, *232*, 233. (b) Wild, F. R. W. P.; Wasiucionek, M.; Huttner, G.; Brintzinger, H. H. *J. Organomet. Chem.* **1985**, *288*, 63.

(15) Representative examples: (a) Lucht, B. L.; Mao, S. S. H.; Tilley, T. D. *J. Am. Chem. Soc.* **1998**, *120*, 4345. (b) Mao, S. S. H.; Liu, F.-Q.; Tilley, T. D. *J. Am. Chem. Soc.* **1998**, *120*, 1193. (c) Takahashi, T.; Hara, R.; Nishihara, Y.; Kortora, M. *J. Am. Chem. Soc.* **1996**, *118*, 5154. (d) Fagan, P. J.; Nugent, W. A.; Calabrese, J. C. *J. Am. Chem. Soc.* **1994**, *116*, 1880. (e) Broene, R. D.; Buchwald, S. L. *Science* **1993**, *261*, 1696.

(16) (a) Negishi, E.; Takahashi, T. *Acc. Chem. Res.* **1994**, *27*, 124. (b) Negishi, E.; Cederbaum, F. E.; Takahashi, T. *Tetrahedron Lett.* **1986**, *27*, 2829. (c) Buchwald, S. L.; Watson, B. T.; Huffman, J. C. *J. Am. Chem. Soc.* **1987**, *109*, 2544.

(17) Dioumaev, V. K.; Harrod, J. F. *Organometallics* **1997**, *16*, 1452, and references therein.

(18) This was also observed in attempts to prepare $(EBI)ZrMe_2$: Rodewald, S.; Jordan, R. F. *J. Am. Chem. Soc.* **1994**, *116*, 4491.

(19) Yoder, J. C.; Day, M. W.; Bercaw, J. E. *Organometallics* **1998**, *17*, 4946, and references therein.

Scheme 2

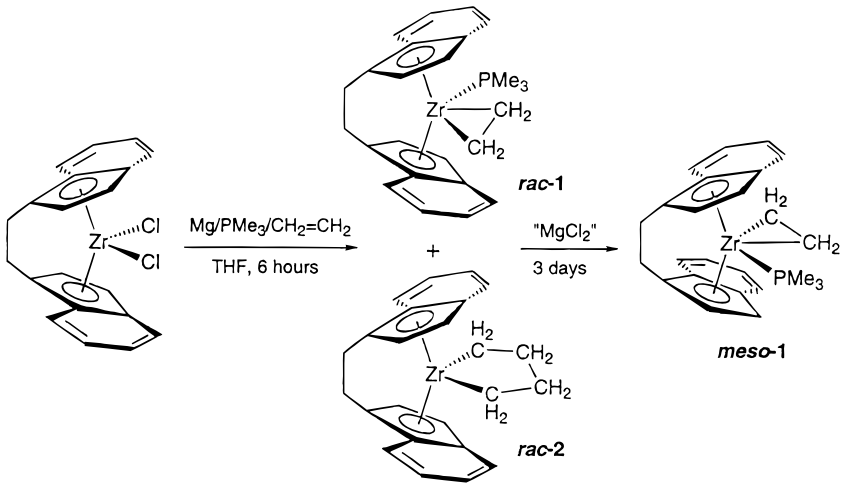

Scheme 3

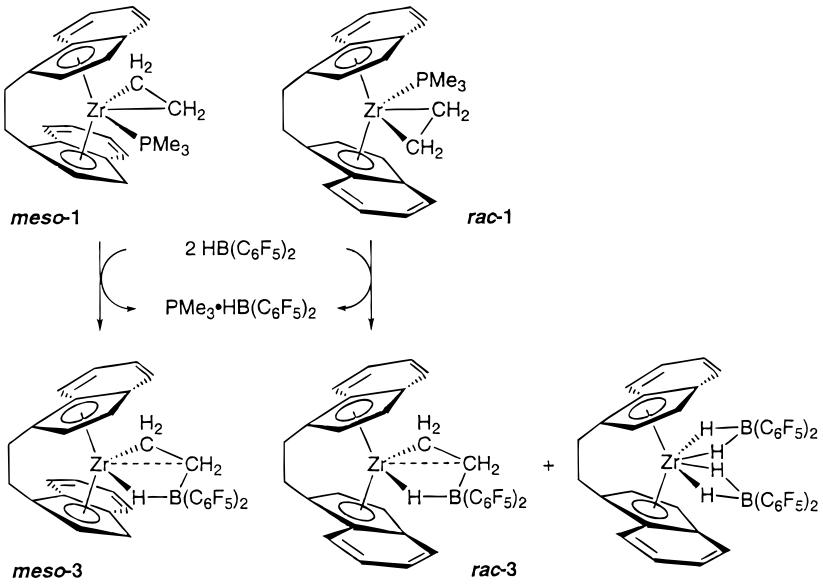

the Experimental Section, samples of diastereomerically pure ***rac*-1** or ***rac*-2** are readily attainable.

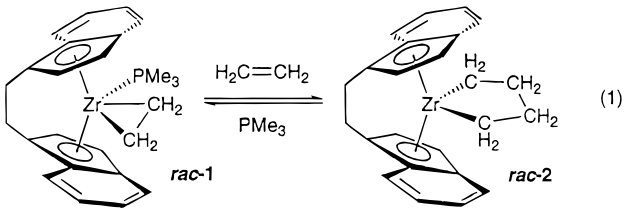

On the other hand, if the magnesium reduction is allowed to stir for 3 days without workup, complete epimerization to the *meso* isomer of **1** is observed. Presumably, this process is mediated by the magnesium salts present. Interestingly, in this system the *meso* diastereomer is the thermodynamic isomer; usually it is the *rac* isomer that is the more thermodynamically stable of the two with this ligand system.[20] At any rate, through careful choice of reaction conditions and timing, diastereomerically pure ***rac*-1** and ***meso*-1** are available for further study.

The new phosphine-stabilized ethylene complexes were fully characterized by multinuclear NMR spectroscopy. Table 1 lists the ^{1}H and $^{13}C\{^{1}H\}$ NMR data for all the new compounds reported herein. In addition, compounds ***meso*-1** and zirconacyclopentane derivative ***rac*-2** were characterized crystallographically. Figures 1 and 2 present the molecular structures of these two derivatives, along with selected metrical data; full details can be found in the Supporting Information.

Both solution and solid-state data show that in ***meso*-1** the ethylene ligand occupies the coordination site sandwiched between the aromatic rings of the indenyl ligands. For example, the chemical shift of the lateral *exo*-CH_2 protons (C(2)) is upfield shifted dramatically to −2.84 ppm as a result of ring current effects[21] from the indenyl rings. As is apparent from the view in Figure 1, the protons of C(2) point nearly directly at the centroids of the indenyl aromatic rings. The open coordination site directed away from the rings

(20) (a) Diamond, G. M.; Jordan, R. F.; Petersen, J. L. *Organometallics* **1996**, *15*, 4030. (b) Diamond, G. M.; Jordan, R. F.; Petersen, J. L. *J. Am. Chem. Soc.* **1996**, *118*, 8024.

(21) Haddon, R. C.; Haddon, V. R.; Jackman, L. M. *Fortschr. Chem. Forsch.* **1971**, *16*, 103.

Table 1. ^{1}H and ^{13}C{^{1}H} NMR Data for Isolated New Compounds[a]

		^{1}H NMR Data			^{13}C{^{1}H} NMR Data	
Compound	#	δ(ppm)	Assignment	J(Hz)	δ(ppm)	Assignment
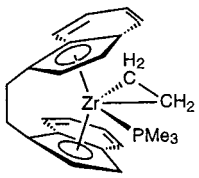	***meso*-1**	7.42, 6.16 (dd, 4H) 6.94, 6.76 (m, 4H) 5.83 (d, 2H) 4.64 (ddd, 2H) 3.31, 2.77 (m, 4H) 0.94 (d, 9H) 0.21 (dt, 2H) -2.84 (t, 2H)	Ar*H* Ar*H* Cp*H* Cp*H* bridge CH_2 PCH_3 *endo*-CH_2 *exo*-CH_2	0.9, 8.6 3.0 0.5, 6.3[b] 5.2[b] 12.0, 6.2[b] 12.0	125.1, 123.9, 121.8, 121.0 97.9, 88.6 122.1, 116.1, 113.2 49.2 36.7 (8.6 Hz[c]) 29.0 18.2 (14.6 Hz[c])	Ar*C* Cp*C*H *Cipso* *exo*-CH_2 *endo*-CH_2 bridge CH_2 PCH_3
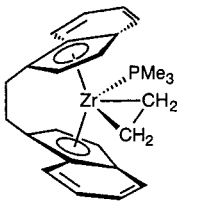	***rac*-1**	7.79, 6.35 (d, 2H) 7.50 (dd, 1H) 7.07 (m, 1H) 6.86 (m, 4H) 6.53, 5.65, 4.00 (d, 3H) 4.47 (dd, 1H) 3.50-2.90 (m, 4H) 0.87 (m, 2H) -0.73, -2.79 (m, 2H) 0.71 (d, 9H)	Ar*H* Ar*H* Ar*H* Ar*H* Cp*H* Cp*H* bridge CH_2 ZrCH_2CH_2 ZrCH_2CH_2 PCH_3	8.6 8.5, 0.7 3.1 3.1, 7.3[b] 5.2[b]	126.7, 124.8, 124.3, 123.6, 120.9, 120.8, 120.1[d] 111.4, 108.8, 88.6, 85.8 ---[e] 45.8, 31.2 30.2, 29.1 15.4	Ar*C* Cp*C*H *Cipso* ZrCH_2CH_2 bridge CH_2 PCH_3
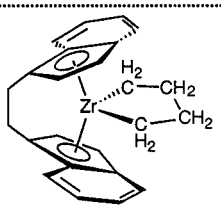	***rac*-2**	7.58, 6.94 (d, 4H) 7.10, 6.86 (m, 4H) 6.76, 5.54 (d, 4H) 2.80-2.50 (m, 4H) 1.86 (m, 2H) 1.53 (m, 4H) -1.92 (m, 2H)	Ar*H* Ar*H* Cp*H* bridge CH_2 ZrCH$_2$CH_2 ZrCH_2CH_2 ZrCH_2	8.5, 8.8 3.2 	125.8, 124.3, 123.9, 120.8 112.3, 105.7 128.8, 124.5, 112.5 51.5 28.3 26.8	Ar*C* Cp*C*H *Cipso* ZrCH_2 ZrCH_2CH_2 bridge CH_2
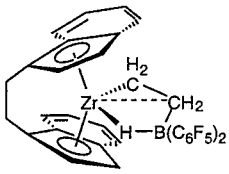	***meso*-3**	7.07, 6.30 (d, 4H) 6.85, 6.75 (m, 4H) 6.08, 5.04 (d, 4H) 3.13, 2.73 (m, 4H) 0.60 (br t, 2H) -0.63 (t, 2H) -1.5 (br, 1H)	Ar*H* Ar*H* Cp*H* bridge CH_2 CH_2B ZrCH_2 Zr*H*B	8.4, 8.6 3.2 9.1 	126.1, 124.6, 124.0, 123.2 111.0, 99.6 122.1, 116.1, 113.2 80.8 28.9 4.3	Ar*C* Cp*C*H *Cipso* ZrCH_2 bridge CH_2 CH_2B
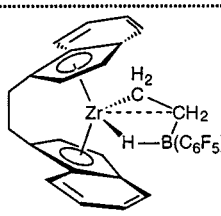	***rac*-3**	7.57, 6.30 (d, 2H) 7.22 (d, 1H) 6.97-6.83 (m, 4H) 5.83 (d, 1H) 5.89, 4.60 (d, 2H) 5.84, 4.97 (d, 2H) 3.37, 3.05, 2.80 (m, 4H) 2.58 (m, 2H) -0.09, -1.76 (m, 2H) -2.5 (br, 1H)	Ar*H* Ar*H* Ar*H* Ar*H* Cp*H* Cp*H* bridge CH_2 ZrCH*H*CH*H*B ZrCH*H*CH*H*B Zr*H*B	7.4, 8.6 8.0 8.0 3.2 2.7 	127.8, 125.2, 124.9, 124.4, 123.9, 123.4, 122.8[d] 113.9, 113.7, 98.4, 97.4 ---[e] 82.5 32.3, 29.9 4.6	Ar*C* Cp*C*H *Cipso* ZrCH_2 bridge CH_2 CH_2B
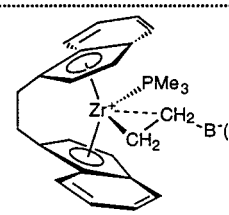	***rac*-4**	7.22, 7.09, 6.92 (d, 3H) 6.81 (m, 1H) 6.72, 6.59 (m, 4H) 5.92, 5.64, 5.09 (d, 3H) 4.81 (dd, 1H) 3.0-2.6 (m, 4H) 1.56, -2.12 (m, 2H) -0.69, -1.66 (m, 2H) 0.40 (d, 9H)	Ar*H* Ar*H* Ar*H* Cp*H* Cp*H* bridge CH_2 ZrCH_2 CH_2B PCH_3	8.6 2.6 2.6, 8.6[b] 7.7[b]	126.2, 125.9, 125.8, 125.2, 125.1, 125.0, 124.3, 122.5 116.9, 107.5, 95.6, 94.9 ---[e] 59.2 31.4, 28.0 4.2 13.9	Ar*C* Cp*C*H *Cipso* ZrCH_2 bridge CH_2 CH_2B PCH_3

[a] All spectra recorded in C_6D_6 unless otherwise noted. [b] J_{PH}. [c] J_{PC}. [d] One resonance obscured. [e] Assignments made by HMQC; quaternary carbons not detected.

is therefore left for the relatively more bulky trimethylphosphine ligand. In ***rac*-1**, the equivalency of each metallocene bonding site dictates that the PMe_3 ligand will have to contend with one indenyl ring when bound to zirconium. This offers an explanation for the greater thermodynamic stability of the *meso* isomer in these less symmetric, essentially triligated *ansa* metallocene systems.

C_s symmetric ***meso*-1** is structurally similar to related compounds. The ethylene ligand is somewhat less symmetrically bound to zirconium than in the parent complexes $Cp_2M(\eta^2\text{-}CH_2{=}CH_2)PMe_3$ (M = Zr,[22] Hf[23]), as evidenced by the relatively disparate Zr−C(1) (2.359(6) Å) and Zr−C(2) (2.282(5) Å) distances. This perhaps disrupts the extent of π-back-bonding, since the C(1)−C(2) distance of 1.424(9) Å, though longer than that of

(22) (a) Alt, H. G.; Denner, C. E.; Thewalt, U.; Rausch, M. D. *J. Organomet. Chem.* **1988**, *356*, C83. (b) Binger, P.; Müller, P.; Benn, R.; Rufinska, A.; Gabor, B.; Krüger, C.; Betz, P. *Chem. Ber.* **1989**, *122*, 1035.

(23) Buchwald, S. L.; Kreutzer, K. A.; Fisher, R. A. *J. Am. Chem. Soc.* **1990**, *112*, 4600.

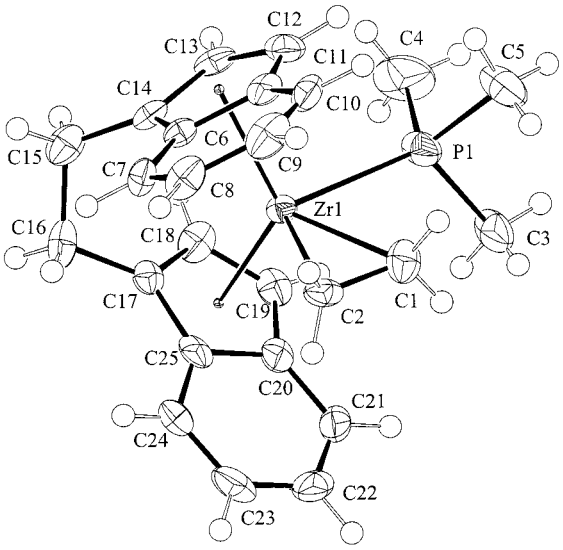

Figure 1. Molecular structure of ***meso*-1**. Selected bond distances, Å: Zr(1)−P(1), 2.667(2); Zr(1)−C(1), 2.359(6); Zr(1)−C(2), 2.282(5); C(1)−C(2), 1.424(9). Selected bond angles, deg: P(1)−Zr(1)−C(1), 75.1(2); P(1)−Zr(1)−C(2), 110.7(2); C(1)−Zr(1)−C(2), 35.7(2); Zr(1)−C(1)−C(2), 69.2(3); Zr(1)−C(2)−C(1), 75.1(4).

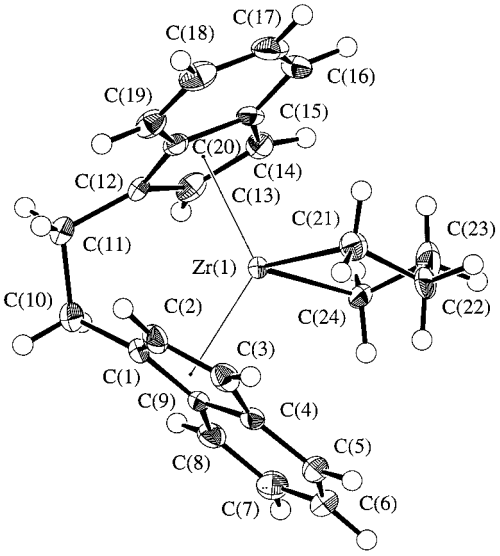

Figure 2. Molecular structure of ***rac*-2**. Selected bond distances, Å: Zr(1)−C(21), 2.305(2); Zr(1)−C(24), 2.282(2); C(21)−C(22), 1.556(4); C(21)−C(22a), 1.543(15); C(22)−C(23), 1.494(4); C(22a)−C(23), 1.424(13); C(23)−C(24), 1.528(3). Selected bond angles, deg: C(21)−Zr(1)−C(24), 84.78(8); Zr(1)−C(21)−C(22), 100.37(15; Zr(1)−C(24)−C(23), 100.10(14; Zr(1)−C(21)−C(22a), 98.3(4); C(21)−C(22)−C(23), 111.5(3); C(22)−C(23)−C(24), 113.5(2); C(21)−C(22a)−C(23), 116.2(11); C(22a)−C(23)−C(24), 125.0(6).

free ethylene (1.337 Å[24]), is slightly shorter than that found in $Cp_2Zr(\eta^2\text{-}CH_2{=}CH_2)PMe_3$ (1.486(8) Å) or the recently reported $\eta^5\text{-}C_5H_3\text{-}1,3\text{-}(SiMe_2CH_2PPr^i{}_2)_2Zr(\eta^2\text{-}CH_2CH_2)Cl$ (1.439(17) Å).[25]

The *rac* isomer of **1** has more complex ^1H and ^{13}C NMR spectra than ***meso*-1** since the unsymmetrical wedge ligation disrupts the C_2 symmetry of the molecule. Thus, separate signals for all protons in the molecule are observed. To fully assign the spectrum, HMQC, COSY, and NOESY 2-D experiments were necessary; the assignments in Table 1 are based on these results. Most notable are the four signals observed for the protons of the ethylene ligand. The high-field signal at −2.79 ppm is ascribed to the *exo* methylene proton pointing into the quadrant occupied by the indenyl ring; other assignments flow from this reference point.

In zirconacyclopentane complex ***rac*-2**, ring currents also affect the chemical shifts observed for the two Zr−CH_2 protons pointing into the indenyl-occupied quadrants; they are shifted to −1.92 ppm compared to a normal shift of ∼1.53 ppm for the α protons which are directed into the empty quadrants of the C_2 symmetric metallocene. The molecular structure of ***rac*-2** (Figure 2) was solved despite a 2-fold disorder at C(22) associated with the conformation of the metallacyclic ring. The compound's metrical properties are similar to other crystallographically characterized zirconacyclopentanes[26] with the exception of the C(21)−Zr−C(24) angle which is about 3° larger at 84.78(8)° than is normally found.

Reactions of *meso*-1 and *rac*-1 with $HB(C_6F_5)_2$. With well-characterized olefin complexes of the ethylenebisindenylzirconium(IV) framework in hand, we turned to examining the reactivity of diastereomers **1** with the two perfluorophenyl-substituted boranes. The course of the reactions of **1** with $HB(C_6F_5)_2$ are similar to that observed in the parent bis-Cp complexes (Scheme 1), producing the hydridoborate-stabilized zwitterions ***meso*-3** and ***rac*-3,** as shown in Scheme 3. As in the bis-Cp system, 2 equiv of borane are required for a clean reaction, one being necessary to soak up the PMe_3 liberated upon ligation of the hydrido borate moiety formed when the H−B bond adds to the Zr−C bond of the coordinated olefin. The *meso* diastereomer could be isolated as an orange solid contaminated with small amounts of the $PMe_3{\cdot}HB(C_6F_5)_2$ byproduct; crystals of this compound were distinguishable from those of the phosphine adduct of $HB(C_6F_5)_2$ via the Pasteur method. Attempts to crystallize ***rac*-3** in the same manner were stymied by a slow decomposition process (vide infra), but the material is stable enough in solution to obtain a complete set of NMR data, which are entirely consistent with the structure given in Scheme 3.

Of the two possible isomers for ***meso*-3**, only the one with the $HB(C_6F_5)_2$ fragment occupying the open side of the metallocene is observed. The situation is therefore analogous to that found in ***meso*-1**, and the explanation is likely also similar; that is, the bulky $B(C_6F_5)_2$ group is more readily accommodated in the open quadrants away from the indenyl rings. As such, the $-CH_2CH_2-$ moiety is again located between these rings, which again have a strong influence on the ^1H NMR chemical shift of the Zr−CH_2 protons. In ***meso*-3**, they resonate at −0.63 ppm. For comparison, the same protons in the bis-Cp system appear at 2.63 ppm.[12a] The protons α to the boron atom are relatively unaffected, appearing at

(24) Bartell, L. S.; Roth, E. A.; Hollowell, C. D.; Kuchitsu, K.; Young, J. E. *J. Chem. Phys.* **1965**, *42*, 2683.

(25) Fryzuk, M. D.; Duval, P. B.; Mao, S. S. H.; Rettig, S. J.; Zaworotko, M. J.; MacGillivray, L. R. *J. Am. Chem. Soc.* **1999**, *121*, 1707.

(26) (a) Taber, D. F.; Louey, J. P.; Wang, Y.; Nugent, W. A.; Dixon, D. A.; Harlow, R. L. *J. Am. Chem. Soc.* **1994**, *116*, 9457. (b) Knight, K. S.; Wang, D.; Waymouth, R. M.; Ziller, J. *J. Am. Chem. Soc.* **1994**, *116*, 1845. (c) Takahashi, R.; Fischer, R.; Xi, Z.; Nakajima, K. *Chem. Lett.* **1996**, 357.

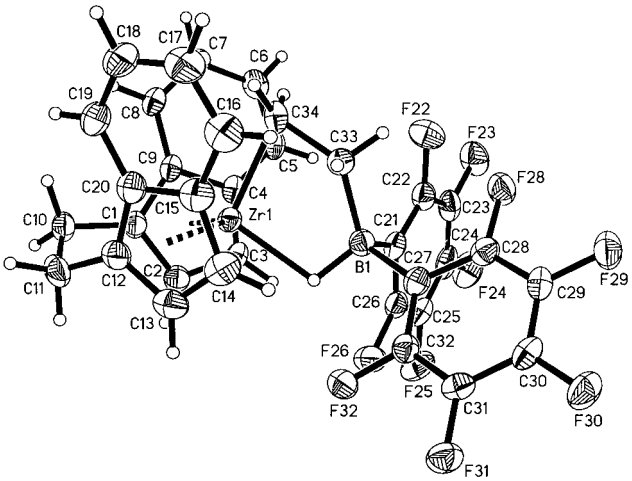

Figure 3. Molecular structure of ***meso*-3**. Selected bond distances, Å: Zr(1)−C(34), 2.199(2); Zr(1)−C(33), 2.494(13); Zr(1)−H(1), 2.01(2); B(1)−C(21), 1.633(4); B(1)−C(27), 1.639(4); B(1)−C(33), 1.721(4); B(1)−H(1), 1.19(2). Selected bond angles, deg: C(34)−Zr(1)−H(1), 102.0(7); C(34)−C(33)−B(1), 126.9(2); C(33)−C(34)−Zr(1), 80.76(14); C(21)−B(1)−C(27), 108.0(2); C(27)−B(1)−C(33), 108.5(2); C(27)−B(1)−H(1), 105.3(11); C(21)−B(1)−C(33), 117.5(2); C(21)−B(1)−H(1), 102.7(11); C(33)−B(1)−H(1), 114.1(12).

0.60 ppm in ***meso*-3** and 0.67 ppm in the parent complex. The high-field chemical shift of the borate CH_2 group in the ^{13}C NMR spectrum (4.3 ppm) is indicative of a weak interaction between this carbon and the zirconium center.[27]

The above points are born out in the solid-state structure of ***meso*-3**. Figure 3 shows a view of this C_s symmetric complex, along with selected bond distances and angles. Particularly noteworthy is the Zr(1)−C(33) distance of 2.494(13) Å, similar to the Zr−C_β distance of 2.455(7) Å found in the bis-Cp analogue.[12a] The acute bond angle for Zr(1)−C(34)−C(33) (80.76(14)°) coupled with the larger than normal values for C(34)−Zr(1)−H(1) (102.0(7)°) and C(34)−C(33)−B(1) (126.9(2)°) illustrates how the five-membered ring comprising H(1), Zr(1), C(34), C(33), and B(1) accommodates the attractive interaction between Zr(1) and C(33).

On the basis of the NMR spectral data accumulated for the isomeric complex ***rac*-3**, the complex probably has a similar structural motif in the wedge portion of the molecule. The ^{13}C chemical shift of 4.6 ppm for the CH_2B carbon atom provides the strongest support for this proposal, although it must be noted that the ^1H NMR spectroscopic data for this grouping are unusual. Given its lack of symmetry elements, the protons of the $-CH_2CH_2-$ fragment are diastereotopic. On the basis of an HMQC experiment, the two protons α to the boron center resonate at −1.76 and ∼2.6 ppm, which are quite different chemical shifts compared to that of ∼0.6 ppm observed for the *meso* isomer and the analogous protons in the bis-Cp system. Its possible that ring current effects are again at play here, particularly if the indenyl groups adopt a twisted conformation about the centroid−metal axis[28] to accommodate the bulky $HB(C_6F_5)_2$ fragment. Certainly the $Zr-CH_2$ protons are again influenced by indenyl ring currents, as evidenced by the disparate chemical shifts of −0.09 and ∼2.6 ppm for these diastereotopic protons.

As mentioned above, neither ***meso*-3** nor ***rac*-3** can be isolated free of $PMe_3{\cdot}HB(C_6F_5)_2$; the latter isomer is also consistently contaminated with a second product of the reaction. When solutions of ***rac*-3** are left standing for several hours, crystals deposit, which, when analyzed by X-ray crystallography, turn out to be the hydridoborate complex $(EBI)Zr[(H)_2B(C_6F_5)_2]_2$.[29] The presence of variable amounts of this complex (10−20%) in crude reactions between ***rac*-1** and $HB(C_6F_5)_2$ is also indicated in the ^{11}B (proton coupled) NMR by a triplet at −13.3 ppm ($^1J_{BH}$ = 67 Hz), similar to data found for the related complex $Cp_2Zr[(H)_2B(C_6F_5)_2]_2$.[30] We have previously noted that $Cp_2Zr\{\eta^3\text{-}[CH_2CH_2BH(C_6F_5)_2]\}$ reacts further with $HB(C_6F_5)_2$ to give $Cp_2Zr[(H)_2B(C_6F_5)_2]_2$ as the major zirconium-containing product.[12a] Similarly, treatment of ***rac*-3** with more borane leads to greater amounts of $(EBI)Zr[(H)_2B(C_6F_5)_2]_2$. The mechanistic details of this chemistry remain obscure.

Reactions of *meso*-1 and *rac*-1 with $B(C_6F_5)_3$. When the EBI ethylene complexes **1** are treated with 1 equiv of $B(C_6F_5)_3$, an immediate red to orange color change is observed, signifying zwitterion formation as indicated for ***rac*-1** in eq 2. In the case of ***meso*-1**, the

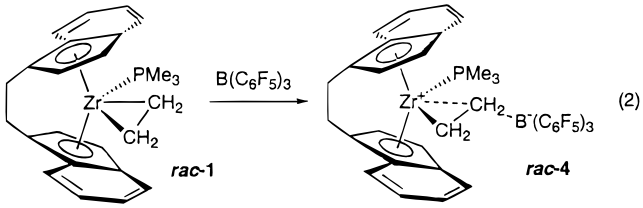

(2)

product oils out of benzene or toluene solution and other minor products are in evidence; clean samples were not obtainable for even rudimentary NMR characterization of the predicted product. For ***rac*-1**, however, the zwitterion ***rac*-4** was formed cleanly and remained in solution long enough to effectively probe by multinuclear NMR spectroscopy. Eventually, crystalline material deposited from these solutions, also allowing for structural analysis of the compound. As seen in Figure 4, ***rac*-4** is formed from $B(C_6F_5)_3$ attack on the centrally ligated *endo* carbon of the coordinated olefin ligand. Despite the lability of the PMe_3 ligand in ***rac*-1**, no $PMe_3{\cdot}B(C_6F_5)_3$[12c,31] is observed in this reaction, and the product zwitterion is stable toward loss of the phosphine adduct, at least over a period of several hours, in solution.

Structurally, ***rac*-4** has several features in common with the bis-Cp analogue we reported earlier.[12b] The hydrogen atoms bonded to C(21) were refined isotropically, and neither C−H bond lies coincident with the

(27) (a) Spence, R. E. v H.; Parks, D. J.; Piers, W. E.; MacDonald, M.; Zaworotko, M. J.; Rettig, S. J. *Angew. Chem., Int. Ed. Engl.* **1995**, *34*, 1230. (b) Radius, U.; Silverio, S. J.; Hoffmann, R.; Gleiter, R. *Organometallics* **1996**, *15*, 3737.

(28) Burger, P.; Diebold, J.; Gutmann, S.; Hund, H.-U.; Brintzinger, H. H. *Organometallics* **1992**, *11*, 1319.

(29) Details of the structural solution for this complex, along with an ORTEP diagram, can be found in the Supporting Information.

(30) Spence R. E. v. H.; Piers, W. E.; Sun, Y.; Parvez, M.; MacGillivray, L. R.; Zaworotko, M. J. *Organometallics* **1998**, *17*, 2459.

(31) This material, if formed, typically appears as a white precipitate in benzene or toluene media. It is almost totally insoluble in these solvents and difficult to detect spectroscopically for that reason.

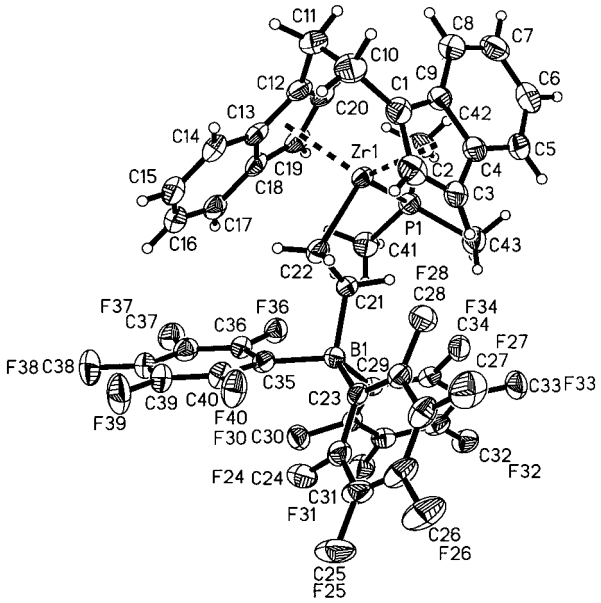

Figure 4. Molecular structure of ***rac*-4**. Selected bond distances, Å: Zr(1)−C(22), 2.250(4); Zr(1)−C(21), 2.570(4); Zr(1)−P(1), 2.7971(11; C(21)−C(22), 1.511(5); B(1)−C(23), 1.656(5); B(1)−C(29), 1.667(6); B(1)−C(35), 1.658(5); B(1)−C(21), 1.685(5). Selected bond angles, deg: C(22)−Zr(1)−P(1), 116.74(10); B(1)−C(21)−Zr(1), 177.3(3); C(22)−C(21)−Zr(1), 60.5(2); C(21)−C(22)−Zr(1), 83.8(2); C(22)−C(21)−B(1), 116.8(3); C(23)−B(1)−C(35), 113.0(3); C(35)−B(1)−C(29), 112.7(3); C(35)−B(1)−C(21), 103.2(3); C(23)−B(1)−C(29), 103.4(3); C(23)−B(1)−C(21), 114.3(3); C(29)−B(1)−C(21), 110.5(3).

metallocene plane; the H atoms are approximately equidistant from zirconium at ∼2.5 Å, arguing against a conventional C−H agostic interaction. However, the relatively close approach of C(21) to the Zr center (Zr(1)−C(21) = 2.570(4) Å) coupled with the small Zr(1)−C(22)−C(21) angle of 83.8(2)° is suggestive of donation of electron density from C(21) to the electropositive zirconium center. The alignment of the B(1)−C(21) vector with the central ligation site of the metallocene (Zr(1)−C(21)−B(1) = 177.3(3)°) along with the nearly perfect coplanarity of Zr(1), C(22), C(21), and B(1) (the dihedral angle comprising these atoms is 179.8(3)°) is consistent with this bonding picture. The C(21) methylene group can be viewed as being an η^3-H−C−H unit similar to that found in the complex $[(C_5H_4Me)_2Zr(CH_2CH_2SiMe_3)(THF)][B(C_6H_5)_4]$.[32] That this structure is likely maintained in solution is supported by the observed C−H coupling constants for the four C−H bonds of the ethylene unit. The values for C_α as determined via an HMQC experiment are 151(1) and 143(1) Hz, consistent with the acute Zr−C−C angle at this carbon,[33] while those for C_β are both 103(1) Hz, suggesting some donation of the σ electron density of these bonds to the zirconium center.[34]

In conclusion, we have developed reliable procedures to diastereomerically pure ethylene complexes of the (EBI)Zr(PMe_3) fragment of both the *rac* and *meso* variety. The reactions of these compounds with the highly electrophilic boranes $HB(C_6F_5)_2$ and $B(C_6F_5)_3$ lead to readily characterizable zwitterions with structural properties similar to those found for the parent biscyclopentadienyl systems we previously reported.

Experimental Section

General Procedures. All operations were performed under a purified argon atmosphere using glovebox or vacuum line teachniques. Toluene, hexanes, and THF solvents were dried and purified by passing through activated alumina and Q5 columns.[35] Dioxane was dried and distilled from sodium benzophenone ketyl. NMR spectra were recorded in dry, oxygen-free C_6D_6, unless otherwise noted. ^{1}H, ^{13}C{^{1}H}, ^{11}B{^{1}H}, ^{19}F, ^{31}P{^{1}H}, HMQC, and NOESY NMR experiments were performed on Bruker AC-200, AMX-300, and WH-400 or Varian 200 MHz spectrometers. Data are given in ppm relative to solvent signals for ^{1}H and ^{13}C spectra or external standards for ^{11}B ($BF_3{\cdot}Et_2O$ at 0.0 ppm), ^{19}F ($CFCl_3$ at 0.0 ppm), and ^{31}P (H_3PO_4 at 0.0 ppm) spectra. Elemental analyses were performed by Mrs. Dorothy Fox of this department. Materials were obtained from Aldrich-Sigma and purified according to standard procedures. Ethylene was purchased from Matheson Gas Products and purified by passing through a Matheson Model DGP-250-R1 Oxyclear purifier cartridge. $B(C_6F_5)_3$ was purchased from Boulder Scientific and dried by stirring with Me_3SiCl prior to vacuum sublimation. *rac*-Ethylenebis(indenyl)zirconium(IV) dichloride[20] and $HB(C_6F_5)_2$[10] were prepared according to literature procedures.

Synthesis of *meso*-(EBI)Zr(η^2-CH_2=CH_2)(PMe_3), *meso*-1. THF (50 mL) was condensed into an evacuated flask containing *rac*-(EBI)$ZrCl_2$ (1.00, 2.39 mmol) and magnesium powder (0.300 g, 12.3 mmol) at −78 °C. An excess (≈5 equiv) of PMe_3 was added via vacuum transfer and the mixture exposed to 1 atm of ethylene. The reaction mixture was slowly warmed to room temperature and stirred for 3 days. The volatiles were removed in vacuo, and fresh THF (25 mL) was condensed into the flask at −78 °C. At room temperature, dry dioxane (5 mL) was added by syringe, and the magnesium salts were removed by filtration. The THF was vacuum evaporated, and the residue was triturated with hexanes (50 mL). Removal of hexanes under vacuum gave ***meso*-1** as a dark red powder. Yield: 720 mg, 64%. ^{31}P{^{1}H} NMR: 4.55 ppm. Anal. Calcd for $ZrC_{25}H_{29}P$: C, 66.48; H, 6.47. Found: C, 66.48; H, 5.66.

Synthesis of *rac*-(EBI)Zr(η^2-CH_2CH_2)(PMe_3), *rac*-1, and *rac*-(EBI)Zr(η^2-$CH_2CH_2CH_2CH_2$), *rac*-2. The same procedure as that described above for ***meso*-1** was followed, except the reaction mixture was stirred for only 6 h. After workup, a red powder containing ***rac*-2**, and ***rac*-1** in a ratio of 1:1 and free from magnesium salts was isolated. This mixture was redissolved in THF (50 mL), exposed to 1 atm of ethylene at room temperature, and stirred for 12 h. The THF was removed under reduced pressure, and the orange residue was recrystallized from hexanes, affording ***rac*-2** as a light orange powder. Yield: 421 mg, 78.8%. Anal. Calcd for $ZrC_{24}H_{24}$ C, 71.41; H, 5.99. Found: C, 70.82; H, 5.53. To prepare ***rac*-1**, ***rac*-2** (0.400 g, 0.887 mmol) was dissolved in benzene and treated with an excess of PMe_3. The reaction mixture was stirred at room temperature for 1 h, cooled to −78 °C, and exposed to vacuum to remove free ethylene. This process was repeated twice. The resulting solution containing ***rac*-1** and traces of ***rac*-2** was stirred for 12 h over a positive pressure of argon. The volatiles were removed under vacuum, and the dark ruby red solid was recrystallized from hexanes. Pure ***rac*-1** was isolated as a ruby red powder in essentially a quantitative yield. ^{31}P{^{1}H} NMR: −1.0 ppm. Anal. Calcd for $ZrC_{25}H_{29}P$: C, 66.48; H, 6.47. Found: C, 62.23; H, 6.03 (average of four analyses).

(32) Alelyunas, Y. W.; Baenziger, N. C.; Bradley, P. K.; Jordan, R. F. *Organometallics* **1994**, *13*, 148.

(33) (a) Yonezawa, T.; Moreshima, I.; Fujii, M.; Fuki, K. *Bull. Chem. Soc. Jpn.* **1965**, ***38***, 1226. (b) Aydin, R.; Gunther, H. *J. Am. Chem. Soc.* **1981**, *103*, 1301.

(34) Brookhart, M.; Green, M. L. H.; Wong, L.-L. *Prog. Inorg. Chem.* **1988**, *36*, 1.

(35) Pangborn, A. B.; Giardello, M. A.; Grubbs, R. H.; Rosen, R. K.; Timmers, F. J. *Organometallics* **1996**, *15*, 1518.

Table 2. Summary of Data Collection and Structure Refinement Details for *meso*-1, *rac*-2, *meso*-3, and *rac*-4

	meso-**1**	*rac*-**2**	*meso*-**3**	*rac*-**4**
formula	$C_{25}H_{29}PZr$	$C_{24}H_{24}Zr$	$C_{34}H_{21}BF_{10}Zr$	$C_{49}H_{35}BF_{15}Zr$
fw	451.70	403.67	721.54	1041.77
cryst syst	orthorhombic	monclinic	monoclinic	triclinic
space group	$P2_12_12_1$	$P2_1/n$	$P2_1$/c	$P\bar{1}$
a, Å	13.612(3)	9.6805(7)	11.2697(1)	11.4417(7)
b, Å	15.154(3)	15.732(3)	17.6728(4)	13.0685(8)
c, Å	10.337(3)	12.1561(4)	14.9759(3)	15.0133(9)
β, deg		105.7779(7)	111.429(1)	106.032(1)
V, Å^3	2132.3(8)	1781.6(3)	2776.51(9)	2157.6(2)
Z	4	4	4	2
d_{calc}, mg m^{-3}	1.407	1.505	1.726	1.604
F(000)	936	832	1440	1048
μ, cm^{-1}	5.97	6.20	4.89	3.93
T, °C	−103	−93	−100	−100
cryst dimens, mm^3	0.50 × 0.40 × 0.20	0.15 × 0.20 × 0.30	0.30 × 0.28 × 0.09	0.38 × 0.25 × 0.10
rel transmiss factors	0.8946−1.0000	0.7302−1.0000	0.713−1.000	0.870−1.000
scan type	$\omega-2\theta$	$\omega-2\theta$		
2θ (max), deg	55.1	60.1		
no. of unique reflns	2807	4662	4882	7214
no. of reflns with $I > n\sigma I$	2123[a]	2934[a]	3827[b]	6558[b]
no. of variables	245	236	419	620
R	0.040	0.050		
R_w	0.040	0.051		
R1			0.0297	0.0361
wR2			0.0753	0.0755
gof	2.12	1.07	0.951	1.040
max Δ/σ (final cycle)	0.00	0.0006		
residual density, e/Å^3	−0.61−0.69	−0.63−0.91	−0.511−0.565	-0.424−0.420

[a] $n = 3$. [b] n = 2.

Synthesis of *meso*-(EBI)Zr{η^3-$CH_2CH_2BH(C_6F_5)_2$}, *meso*-3. Toluene (20 mL) was condensed into an evacuated flask containing ***meso*-1** (65 mg, 0.144 mmol) and $HB(C_6F_5)_2$ (100 mg, 0.288 mmol) at −78 °C. The brown-orange mixture turned yellow as the solution slowly warmed to room temperature. Stirring was continued for another 30 min. The toluene was removed under vacuum, and the yellow residue was triturated with hexanes. The solid was isolated by filtration and washed twice with hexanes to remove as much of the $HB(C_6F_5)_2{\cdot}PMe_3$ as possible. The yellow solid thus isolated was comprised mainly of ***meso*-3** contaminated with traces of $HB(C_6F_5)_2{\cdot}PMe_3$. $^{11}B\{^1H\}$ NMR: −0.5 ppm. ^{19}F NMR: −131.6, F_{ortho}; −157.2, F_{para}; −162.9, F_{meta}. Analytically pure samples were not obtainable.

Synthesis of *rac*-(EBI)Zr{η^3-$CH_2CH_2BH(C_6F_5)_2$}, *rac*-3. The preparation of ***rac*-3** followed a similar method as ***meso*-3** with the exception that ***rac*-1** (100 mg, 0.222 mmol) and $HB(C_6F_5)_2$ (153 mg, 0.443 mmol) were used. Attempts to grow X-ray quality crystals of ***rac*-4** by slow evaporation of a benzene solution resulted in the isolation of X-ray quality crystals of *rac*-(EBI)Zr[$(H)_2B(C_6F_5)_2]_2$. ^{11}B NMR: 3.4 (d, $^1J_{BH}$ = 66 Hz). ^{19}F NMR: −131.8, −130.5, F_{ortho}; −157.6, F_{para} (other *para* resonance obscured by byproduct signals); −162.6, −165.9, F_{meta}.

Synthesis of *rac*-Zr(EBI){$CH_2CH_2B(C_6F_5)_3$}, *rac*-4. A solution of $B(C_6F_5)_3$ (23 mg, 0.045 mmol) in 0.5 mL of C_6D_6 was added slowly to a solution of ***rac*-1** (20 mg, 0.044 mmol), also in C_6D_6, with constant agitation. The resulting sample was filtered through a plug of Celite into an NMR tube and assayed spectroscopically. From such a sample, X-ray quality crystals of ***rac*-4** were deposited and analyzed. Attempts to prepare ***rac*-4** on a preparative scale resulted in the isolation of an orange oily material comprised largely of ***rac*-4**, but not analytically pure. $^{31}P\{^1H\}$ NMR: −17.6 ppm. $^{11}B\{^1H\}$ NMR: −12.3 ppm. ^{19}F NMR: −130.6, F_{ortho}; −161.3, F_{para}; −165.3, F_{meta}.

X-ray Crystallography. A summary of crystal data and refinement details for all structures is given in Table 2. Suitable crystals were covered in paratone oil, mounted on a glass fiber, and immediately placed in a cold stream on the diffractometer employed.

***meso*-1.** Crystals of ***meso*-1** were grown from toluene/hexanes solution at room temperature. Measurements were made using a Rigaku AFC6S diffractometer with a graphite-monochromated Mo Kα radiation (λ = 0.71069 Å) source at −103 °C with the $\omega-2\theta$ scan technique to a maximum 2θ value of 55.1°. The structure was solved by direct methods and refined by full-matrix least-squares calculations. The non-hydrogen atoms were refined anisotropically; hydrogen atoms were included at geometrically idealized positions with C−H = 0.95 Å and were not refined. All calculations were performed using the TEXAN[36] crystallographic software package of Molecular Structure Corporation.

***rac*-2.** Crystals of ***rac*-2** were grown from toluene/hexanes solution at room temperature. Measurements were made using a Rigaku/ADSC CCD area detector with a graphite-monochromated Mo Kα radiation (λ = 0.71069 Å) source at −93 °C with the $\omega-2\theta$ scan technique to a maximum 2θ value of 60.1°. The structure was solved by heavy-atom Patterson methods and expanded by full-Fourier techniques. The population parameter of the major component was refined, and that of the minor component (C(22a)) was fixed at 1.0 − pop(C(22)). The non-hydrogen atoms were refined anisotropically, while hydrogen atoms were included at calculated positions with C−H = 0.98 Å and were not refined. All calculations were performed using the TEXAN crystallographic software package.

***meso*-3.** Yellow crystals of ***meso*-3** were grown from toluene by slow evaporation and selected from among clear crystals of $PMe_3{\cdot}HB(C_6F_5)_2$ for mounting on a glass fiber. Measurements were made on a Siemens SMART system at 173(2) K using a hemisphere data collection technique in which a randomly oriented region of reciprocal space was surveyed to the extent of 1.3 hemispheres to a resolution of 0.84 Å. Three swaths of frames were collected with 0.30° steps in ω. The structure was solved by direct methods. The non-hydrogen atoms were refined with anisotropic displacement parameters. All hydrogen atoms except the bridging hydrogen atom, H(1), were placed in ideal positions and refined as riding atoms with

(36) Crystal Structure Analysis Package; Molecular Structure Corporation, 1985 and 1992.

relative isotropic displacement parameters. H(1) was refined as an isotropic atom.

***rac*-4.** Crystals of ***rac*-4** were grown from benzene solution and mounted on a glass fiber. Data collection procedures were identical to that described for ***meso*-3** above. The non-hydrogen atoms were refined with anisotropic displacement parameters. The majority of hydrogen atoms were placed in ideal positions and refined as riding atoms with relative isotropic displacement parameters. The hydrogen atoms on C(21) and C(22) were refined isotropically with relative isotropic displacements.

All calculations concerning the structure refinements for ***meso*-3** and ***rac*-4** were performed using SGI INDY R4400−SC or Pentium computers using the SHELXTL V5.0 suite of programs.

Acknowledgment. This work was generously supported by the NOVA Research & Technology Corporation of Calgary, Alberta, and NSERC of Canada's Research Partnerships office (CRD program). W.E.P. thanks the Alfred P. Sloan Foundation for a Research Fellowship (1996-2000).

Supporting Information Available: Tables of atomic coordinates and isotropic thermal parameters, bond lengths and angles, H atom coordinates, and anisotropic thermal parameters for compounds ***meso*-1**, ***rac*-2**, ***meso*-3**, ***rac*-4**, and $(EBI)Zr[(H)_2B(C_6F_5)_2]_2$. This material is available free of charge via the Internet at http://pubs.acs.org.

OM990383D